Journal of Materials and Engineering Structures

Research Paper

Stress in closed thin-walled tubes of single box subjected by shear forces and application to airfoils

Boun-jad Mohamed [a]***, Zebbiche Toufik*** [a]****, Allali Abderrazak*** [b]

[a]*Aeronautical Science Laboratory, Institute of Aeronautics and Space Studies, University of Blida 1, Algeria*

[b]*Aircraft Laboratory, Institute of Aeronautics and Space Studies, University of Blida 1, Algeria*

ARTICLE INFO

Article history :

Received : 17 April 2014

Revised : 15 July 2014

Accepted : 26 July 2014

Keywords:

Thin Wall

Shear center

Shear stress

Airfoil section

ABSTRACT

The presented work is to develop a numerical computation program to determine the distribution of the shear stress in closed tubes with asymmetric single thin wall section with a constant thickness and applications to airfoils, and therefore determining the position and value of the maximum stress. In the literature, there are exact analytical solutions only for some sections of simple geometries such as circular section. Hence our interest is focused on the search of approximate numerical solutions for more complex sections used in aeronautics. In the second stage the position of the shear center is determined so that the section does not undergo torsion. The analytic function of the airfoil boundary is obtained by using the cubic spline interpolation since it is given in the form of tabulated points.

1 Introduction

The calculation of the shear stress in sections of thin-walled tubes, in particular the geometry of an airfoil coating play a very important role in the calculation of elasticity [1] and [2]. When the section is subjected to one or two shear forces, the section will be loaded by a shear stress along the boundary [1] and [2]. For an aerospace vehicle, most of the structures of the materials are manufactured by the thin wall. We talk about the wing, fuselage shell, drift, tail, rails, helicopter blade, etc. [1] and [2]. It determines the distribution of shear stress in order to locate the maximum stress with its value for not having a break caused by the shear forces. During movement of the aerospace vehicle there will be a pressure distribution on the exit surface of the craft. This distribution generally gives an aerodynamic torsor formed by three forces and three moments. In a plane section the torsor is formed by two forces one horizontal and the other vertical and a pitching moment

* *Corresponding author. Tel.: +213 (0) 662197226*
E-mail address: z_toufik270169@yahoo.fr

RESEARCH REVIEW of Sciences and Technologies

e-ISSN: 2170-127X,

[1] and [2]. These external forces are transformed into internal forces. Where the horizontal and vertical shear forces births S_x and S_y and a vertical pitch moment present as T in Figure 1. These internal forces are themselves therefore gives a distribution of shear stress along the coating.

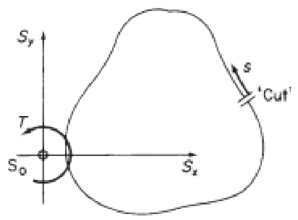

Fig. 1 - Shear of closed tube section and presentation of the opening section.

In this first publication we are interested only in the sections formed by a single box. Sections formed by two or more boxes are left for future publications.

This work is then to develop a numerical computation program to determine the distribution of the shear stress of the shear force in any closed thin-wall tubes, of one box having a constant thickness and to make applications to airfoils, for aim to determine the position and the value of the maximum stress. Given the complexity of the section, the calculation is purely numerical. In other words, the exact solution does not exist.

The calculation is made by the discretization of the boundary that will be considered by straight line segments. The segments are defined by their positions of these two nodes. Our application is limited to thicknesses well below the unit t/C <0.01. Usually in the actual case, the value of it, is of the order of millimeters around 1 to 2 mm [1] and [2].

To determine the distribution of shear stress in closed sections, it is first necessary to cut the section in a point of the boundary, to be the trailing edge for example. The same results will be found if the position of the cutting is changed. The difference between a closed and the open section is that we must determine the value of the stress at the opening that will be added to the stress at each point of the open section.

Because the number of segments is very important, the calculation becomes numerical. The accuracy of the calculation depends on the discretization. More the number of segments increases, there will be a good accuracy.

Generally boundary of airfoil is given as tabulated points [3], so we have to interpolate them, to determine an analytical form of the geometry [5] and [6]. Interpolation chosen is the cubic spline [5]. Among the advantages of this method, it keeps the curvature of the airfoil at the leading edge.

2 Shear Flow in open section

To start the calculation, it is necessary to cut the section in any place like in Figure 1 [1] and [2]. The value of the shear flow at this point is zero for the open section. We chose to make the opening at the trailing edge. A segment of the boundary is presented by its end nodes as presented in Figure 2. The coordinates of nodes i and j are known from the mark passing through the center of gravity. The numbering of nodes is done in a counter clockwise direction starting from the trailing edge

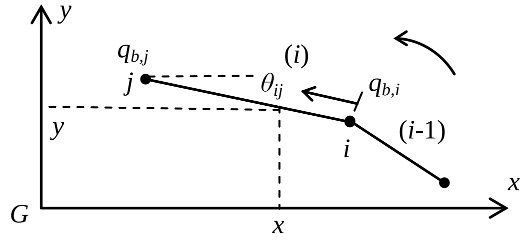

Fig. 2 - Introducing the segment calculation

Value of the shear flow at a point (x, y) of the segment number (i) of Figure 2 for the case of open section having a constant thickness is given by:

$$q_{b,ij}(s)=q_{b,i}-H_1\int_0^s x\,ds-H_2\int_0^s y\,ds \tag{1}$$

Shear stress τ is connected with the shear flow by the following relationship [1] and [2];

$$\tau=\frac{q}{t} \tag{2}$$

with

$$H_1=t\left(\frac{S_x I_{xx}-S_y I_{xy}}{I_{xx}I_{yy}-I_{xy}^2}\right),\quad H_2=t\left(\frac{S_y I_{yy}-S_x I_{xy}}{I_{xx}I_{yy}-I_{xy}^2}\right) \tag{3}$$

The moments of inertia I_{xx}, I_{yy} and product of inertia I_{xy} must be calculated relative to a central axis of the section. For more details, consult the references [7].

From Figure 3, we can write:

$$x=x_i-\frac{x_i-x_j}{L_{ij}}s,\quad y=y_i-\frac{y_i-y_j}{L_{ij}}s \tag{4}$$

with

$$L_{ij}=\sqrt{(x_i-x_j)^2+(y_i-y_j)^2} \tag{5}$$

Substituting the relations (4) into (1) and integrating, we obtain:

$$q_{b,ij}(S)=q_{b,i}-H_1\left(x_i\,s-\frac{x_i-x_j}{2\,L_{ij}}s^2\right)-H_2\left(y_i\,s-\frac{y_i-y_j}{2\,L_{ij}}s^2\right) \tag{6}$$

Where

$$q_{s,ij}(S)=q_{b,ij}(S)+q_{s,0} \tag{7}$$

According to equation (6), a parabolic distribution of shear flow along the segment length can be seen. From equation (6), the value of shear flow at the point j is obtained when s = L_{ij}. We obtain:

$$q_{b,j}=q_{b,i}-H_1\,L_{ij}\frac{x_i+x_j}{2}-H_2\,L_{ij}\frac{y_i+y_j}{2} \tag{8}$$

In equation (7), i=1, 2, 3, ..., NS-1 and j=i+1. The total shear flow point j is calculated by adding the shear flow of the opening section. Then

$$q_{s,j}=q_{b,j}+q_{s,0} \tag{9}$$

For i=1, the shear flow at the point of the opening is equal to zero. Then

$$q_{b,1}=0 \tag{10}$$

3 Determining the value of qs,0

The values of $q_{s,0}$ represents the shear flow at the point of the opening. This calculation is made by the following equation [1] and [2]:

$$q_{s,0}=-\frac{\oint q_b\,ds}{\oint ds} \tag{11}$$

This value represents the average value of shear flow. In relation (11), the denominator can be approximated by:

$$\oint ds = L = \sum_{i=1}^{i=NS} L_{ij} \tag{12}$$

The result in equation (12) is made by the sum of the lengths of all the segments constituting the discretization. According to equation (11) we can write again:

$$\oint q_b\, ds = \sum_{i=1}^{i=NS} \int_0^{L_{ij}} q_{b,ij}(s)\, ds \tag{13}$$

Replacing equation (6) into (13) and integrating we obtain after a rearrangement result, which will be replaced in equation (11) we obtain the final result for $q_{s,0}$. Then:

$$q_{s,0} = -\frac{1}{L}\sum_{i=1}^{i=NS}\left[q_{b,i}L_{ij} - H_1 L_{ij}^2 \frac{2x_i + x_j}{6} - H_2 L_{ij}^2 \frac{2y_i + y_j}{6}\right] \tag{14}$$

Therefore one can determine the value of stress at the opening by the following relationship:

$$\tau_{s,0} = \frac{q_{s,0}}{t} \tag{15}$$

Replacing the result given by equation (14) into equation (9), we can obtain the total value of shear flow at each point of the discretization.

In equations (12), (13) and (14), j=i+1. If i=NS, then j=1. In relation (14), more the number of segments is high, the more we will have a good precision.

Once one determines the distribution of the shear flow by the equation (9), one can easily deduce the distribution of shear stress using the relationship (2).

In the end we can determine the value and the position of the maximum shear stress. We can have two values of maximum stress. One for the positive values and the other for negative values. It is necessary that these values are lower than the allowable stress τ_{ad}^{+} and τ_{ad}^{-} for not having a break.

4 Shear center

To eliminate the torsion caused by cutting efforts, it is very interesting to apply these efforts in a sharp point called shear center. The determination of this point is in relation to any point. In our study we have chosen the leading edge of the airfoil to calculate the moment.

The position of the shear center of closed thin wall beams is located in the same way as open tubes [1] and [2]. However, for determining the position of the shear center of coordinates (ξS, ηS) of the thin-walled closed beam shown in Figure 3, we arbitrarily apply a distribution of, shear horizontal Sx and vertical shear Sy at the point S. Then we calculate the shear flow qs of the sharp stress and then tying the internal moment to external moment. But at this level, it is impossible to equalize the internal moment of the shear flow to the moment of external shear forces for an equation as Shear Force Sx and Sy are unknown. For the solution, provided that the shear forces are applied to the shear center to produce a zero moment applied.

The calculation is done by the following equation [1] and [2]:

$$\xi_S S_y \text{-} \eta_S S_x = \oint d\, q_S ds \tag{16}$$

For the calculation was chosen counterclockwise from the point O. In equation (16), the symbol d represents the value of the lever arm of the point of application of shear flow q_S. For a discretization of NS segments on the boundary as presented in Figure 6, the relation (16) becomes:

$$\xi_S S_y \text{-} \eta_S S_x = \sum_{i=1}^{i=NS} d_{ij} \int_0^{L_{ij}} q_{S,ij}(s)ds \tag{17}$$

The d_{ij} value in equation (17) represents the lever arm of the segment connecting the nodes i and j as presented in Figure 4. In this case, to determine the value of d, we must first determine the equation of the line connecting the points i and j and the equation of the straight line perpendicular to the line connecting the points i and j, and passes through the point O. The intersection of these two lines gives the position of the point k as presented in Figure 6. We can consequently determine the distance between the points O and k representing the distance d_{ij}. Then:

$$y_{ij}(x) = \frac{y_j - y_i}{x_j - x_i}(x - x_i) + y_i \tag{18}$$

and

$$y_{ok}(x) = -\frac{x_j - x_i}{y_j - y_i}(x - x_O) + y_O \tag{19}$$

The position of O (x_O, y_O) is given. Evening now the ordered of equations (18) and (19), we can obtain the position of point k by :

$$x_k = \frac{y_O - y_i + \frac{x_j - x_i}{y_j - y_i}x_O + \frac{y_j - y_i}{x_j - x_i}x_i}{\frac{y_j - y_i}{x_j - x_i} + \frac{x_j - x_i}{y_j - y_i}} \tag{20}$$

$$y_k = -\frac{y_j - y_i}{x_j - x_i}(x_k - x_i) + y_i \tag{21}$$

Therefore, the distance d_{ij} between the points O and k is calculated by the following equation:

$$d_{ij} = \sqrt{(x_k - x_O)^2 + (y_k - y_O)^2} \tag{22}$$

We preferred to introduce the indices i and j instead the indices O and k for calculating the value of the lever arm of the segment connecting between the nodes i and j. Replacing the equation (7) in equation (17) and integrating along the segment connecting the nodes i and j we get the following result:

$$\xi_S S_y \text{-} \eta_S S_x = \sum_{i=1}^{i=NS} d_{ij}\left[q_{b,i}\, L_{ij} + q_{s,0}\, L_{ij} - H_1 \frac{L_{ij}^2}{6}\left(2\,x_i + x_j\right) - H_2 \frac{L_{ij}^2}{6}\left(2y_i + y_j\right)\right] \tag{23}$$

In equation (23) expressions d_{ij}, $q_{b,i}$, $q_{S,0}$, H_1, H_2 and L_{ij} are given respectively by the relations (22), (8), (14), (3) and (5). The positions of nodes i and j are given.

From equation (23) to determine the abscissa ξ_S of the the shear center, we take S_x=0.0 and and S_y arbitrary. In the computer program, we took S_y=1.0. To determine the value η_S of the shear center, we set S_y=0.0 and S_x arbitrary. In the calculation program was given S_x=1.0.

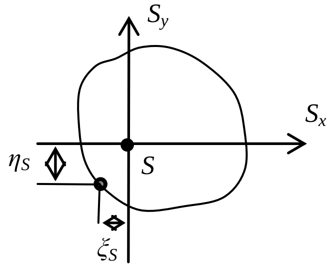

Fig. 3 - Shear center of a closed section.

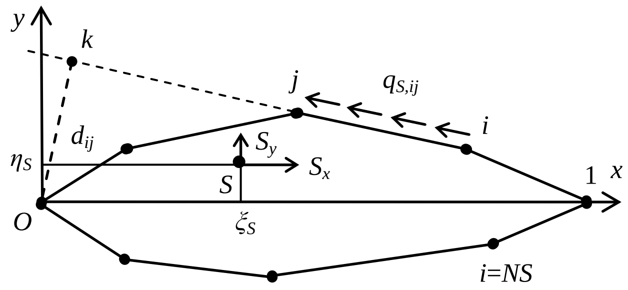

Fig. 4 - Schemes for calculating shear center.

5 Mesh generation

It should be noted that the geometry of the airfoil is given as tabulated values. So we used the cubic spline interpolation to find an analytical equation of the upper and lower surface. The number of points selected for the mesh generation is different from that given for the definition of the geometry of the airfoil. The resulting mesh is formed by straight line segments placed on the boundary of the airfoil as presented in Figures 6, 7, 8, 9, 10 and 11.

5.1 Stretching function

Due to the curvature of the boundary, it is sometimes used to condense the nodes into a well specified to have a good presentation of the boundary, particularly at the leading edge for the subsonic airfoils, where there is a district area in the boundary [4].

If the stretching function is applied to the EA side (see Figure 5), for example, on the airfoil chord, the standardized independent variable is given by:

$$\eta^* = \frac{\eta - \eta_A}{\eta_E - \eta_A} \tag{24}$$

with : $0 \le \eta^* \le 1$ and $\eta_A \le \eta \le \eta_E$

where: η may represent x

We can even give the distribution on the interval [0, 1] by η^* with equal sub-intervals.

The stretching function used is given by [4]:

$$s = P\ \eta^* + (1 - P)\left[1 - \frac{\tanh\left[Q(1-\eta^*)\right]}{\tanh\left[Q\right]}\right] \tag{25}$$

Once the value of s is obtained, it is required to specify the distribution of x. for example

$$x = x_A + s\ (x_A - x_E) \tag{26}$$

For values of P>1.0, it is possible to condense the nodes to point A.

Typical distributions of points on the EA segment for different values of P and Q, are shown in the following figure 7:

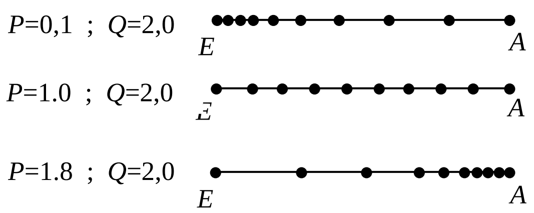

***Fig. 5* - Distribution of nodes according to equation (25).**

To obtain the ordinate of the point considered on the boundary, it is sufficient to use the analytic function of the upper or lower surface of the airfoil.

5.2 Connecting segments of the mesh

The numbering of the nodes of the mesh starts with the trailing edge in the counter clockwise direction. If the number of points on the boundary is *NN*, then the number of segments treated equals *NS*=*NN*.

The problem is to assemble these segments to get the result for the entire section. To get results, we must have to know the numbers of nodes of each segment, see Figure 3. For the number (i) (i = 1, 2, 3, ..., *NN*), the node j=i +1. For the last segment, the number of node j=1 (closed boundary). This segment is in the lower surface with a node that is the trailing edge.

6 Results and comments

In Figures 6, 7, 8, 9, 10 and 11 mesh chosen in our calculation. It is formed by segments of the boundary. We took the following parameters P=1.9, Q=2.00 for the upper surface and P=0.01, Q=2.00 for the lower surface. The airfoil selected in these figures is the DOUGLAS LA203A unsymmetrical with camber. The definition of the geometry is presented by 51 points as Table 1 shows [3].

Note that the numbering of the nodes on the upper begins from the trailing edge to the leading edge whereas for the lower surface, the numbering of nodes starts from leading edge to the trailing edge. The mesh is made so that there is condensation of nodes to the leading edge to see the curvature. This procedure is especially important for subsonic and transonic airfoil.

In these figures were taken respectively *NS*=15, 30, 60, 100, 200 and 350 segments of the boundary to see the position of the nodes. Note that the developed program can make unlimited mesh presentation. For applications, we took the number of segments to one Million.

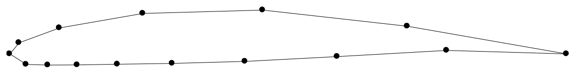

Fig. 6 **- Discretization of the boundary of the airfoil by NS=15.**

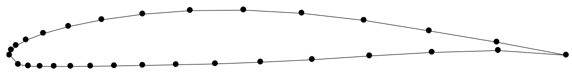

Fig. 7 **- Discretization of the boundary of the airfoil by NS=30.**

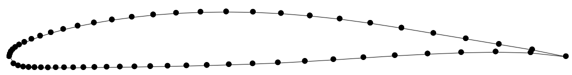

Fig. 8 **- Discretization of the boundary of the airfoil by NS=60.**

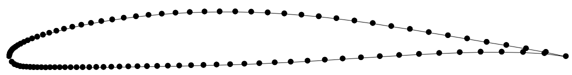

Fig. 9 **- Discretization of the boundary of the airfoil by NS=100.**

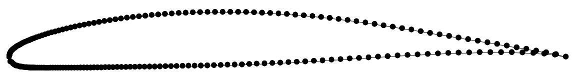

Fig. 10 **- Discretization of the boundary of the airfoil by NS=200.**

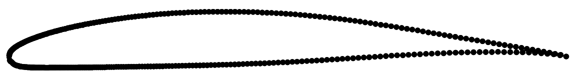

Fig. 11 **- Discretization of the boundary of the airfoil by NS=350.**

Table 1 - Defining points of the surface of the airfoil DOUGLAS LA203A.

		Upper surface In (%) of C	Lower surface In (%) of C
	x/C (%)	y/C (%)	y/C (%)
01	0.0000	0.0000	0.0000
02	0.0887	0.6000	-0.8018
03	0.3544	1.5836	-1.5137
04	0.7963	2.3336	-2.1544
05	1.4127	3.0677	-2.6516
06	2.2015	3.8031	-2.9638
07	3.1599	4.5492	-3.1320
08	4.2846	5.3047	-3.2209
09	5.5715	6.0636	-3.2676
10	7.0162	6.8190	-3.2867
11	8.6135	7.5641	-3.2657
12	10.3579	8.2919	-3.2692
13	12.2432	8.9956	-3.2407
14	14.2628	9.6688	-3.2024
15	16.4095	10.3048	-3.1557
16	18.6758	10.8970	-3.1016
17	21.0538	11.4389	-3.0405
18	23.5350	11.9234	-2.9724
19	26.1106	12.3424	-2.8967
20	28.7718	12.6854	-2.8125
21	31.5090	12.9435	-2.7184
22	34.3127	13.1182	-2.6124
23	37.1729	13.2075	-2.4919
24	40.0796	13.2090	-2.3512
25	43.0226	13.1219	-2.1826
26	45.9916	12.9436	-1.9830
27	48.9759	12.6743	-1.7533
28	51.9653	12.3176	-1.4947
29	54.9490	11.8770	-1.2099
30	57.9167	11.3566	-0.9052
31	60.8579	10.7640	-0.5917
32	63.7621	10.1087	-0.2822
33	66.6193	9.4063	0.0143
34	69.4194	8.6797	0.2917
35	72.1524	7.9995	0.5448
36	74.8087	7.2292	0.7686
37	77.3791	6.5291	0.9596
38	79.8545	5.8545	1.1145
39	82.2261	5.2086	1.2313
40	84.4856	4.5936	1.3087
41	86.6250	4.0113	1.3484
42	88.6369	3.4630	1.3448
43	90.5141	2.9490	1.3056
44	92.2500	2.4700	1.2302
45	93.8385	2.0258	1.1218
46	95.2740	1.6162	0.9838
47	96.5516	1.2408	0.8211
48	97.6665	0.8985	0.6392
49	98.6151	0.5883	0.4425
50	99.3938	0.3044	0.2384
51	100.0000	0.0000	0.0000

The points of the table 1 are used to determine the analytical function of the extrados and intrados, using cubic spline interpolation.

6.1 Effect of discretization on the convergence

We will justify the convergence of the numerical results to the exact solution by making the change in the number of segments on the section and see the convergence of the calculation parameters $\tau_{s,0}$, $\tau^+_{\max}$, $\tau^-_{\min}$, ξ_S, η_S. Taking the example of a circle of radius R=1.0. The center located at the point xG=R, yG=0.0 as presented in Figure 12. For this example we took t=0.01. In this case, the values of the moments and product of inertia with respect to the central axis (horizontal and vertical) are given by [7]:

$$I_{xx}/(R^3t) = I_{yy}/(R^3t) = 3.1415926535 \tag{27}$$

$$I_{xy} = 0.0 \tag{28}$$

The values of $\tau_{s,0}$, $\tau^+_{\max}$, $\tau^-_{\min}$, ξ_S, η_S for some values of number of segments are presented in tables 2 and 3. In these tables, we took Sx=1.0 and Sy=1.0. Note that $\tau_{s,0}$, $\tau^+_{\max}$, $\tau^-_{\min}$ depend on Sx and Sy, and that ξ_S, η_S do not depend on Sx and of Sy.

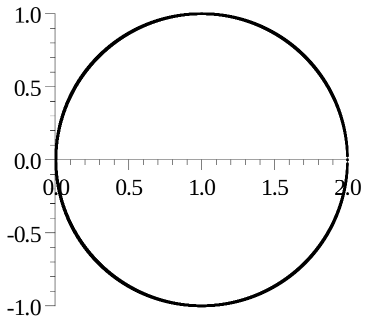

Fig. 12 - Presentation of the thin-walled circle.

Table 2 - Effect of discretization on the convergence of $\tau_{s,0}$, $\tau^+_{\max}$ et $\tau^-_{\min}$ for the circle.

NS	$\tau_{s,0}$	$\tau^+_{\max}$	$\tau^-_{\min}$
10	32.120821	46.114908	-47.060181
20	31.830346	45.893652	-46.075668
50	31.837888	45.178012	-45.306287
100	31.839597	45.059774	-45.121430
200	31.836513	45.021131	-45.051751
300	31.834777	45.019860	-45.036059
500	31.833184	45.018975	-45.025069
700	31.832476	45.017202	-45.021673
1000	31.831951	45.016513	-45.019245
2000	31.831394	45.016210	-45.017048
5000	31.831112	45.015888	-45.016115
8000	31.831075	45.015874	-45.015984
10000	31.831064	45.015860	-45.015940
20000	31.831020	45.015832	-45.015853
50000	31.830997	45.015824	-45.015826
10^5	31.830993	45.015823	-45.015824
10^6	31.830992	45.015823	-45.015823

In Figures 13, 14, 15, 16 and 17 were presented respectively the variation of parameters $\tau_{s,0}$, $\tau^{+}_{\max}$, $\tau^{-}_{\min}$, ξ_S, η_S depending on the number of segments to see the convergence of these parameters to the exact solution. We see clearly from this figure and tables 2 and 3, the convergence of these parameters. It is present setting decimal digits, plus the number of segments increases, which interprets the convergence settings to the exact solution. Stability occurs for the parameters from NS=300 segments. So to have an accuracy of ε=10-3, we have about 300 segments. For a precision ε=10-6, it takes about 40000 segments.

Table 3 - Effect of discretization on the convergence of values ξ_S et η_S for the circle.

NS	ξ_S	η_S
10	0.8899922873	0.0383217545
20	0.9543224561	0.0041862997
50	0.9868014410	0.0000310035
100	0.9950410087	-0.0000623843
200	0.9981762532	-0.0000273174
300	0.9989907237	-0.0000144579
500	0.9995234514	-0.0000060630
700	0.9997101922	-0.0000033406
1000	0.9998296578	-0.0000017599
2000	0.9999398717	-0.0000004839
5000	0.9999860454	-0.0000000820
8000	0.9999931018	-0.0000000322
10000	0.9999951684	-0.0000000255
20000	0.9999986939	-0.0000000034
50000	0.9999999355	-0.0000000007
10^5	0.9999999834	-0.0000000004
10^6	1.0000000000	0.0000000001

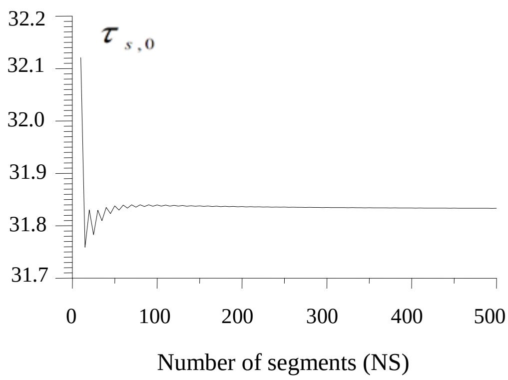

Fig. 13 - Variation of $\tau_{s,0}$ versus the number of segments NS for the circle.

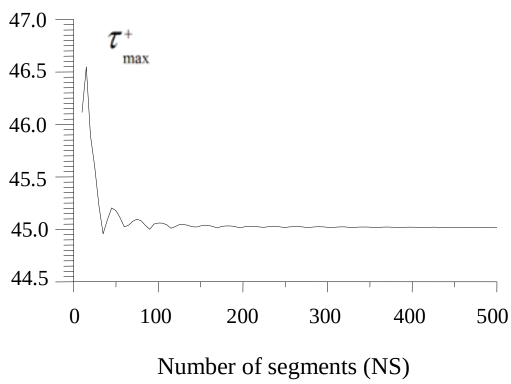

Fig. 14 - Variation of $\tau^{+}_{\max}$ versus the number of segments NS for the circle.

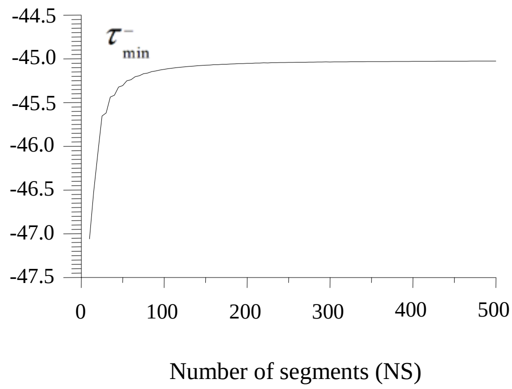

Fig. 15 - Variation of $\tau^{-}_{\min}$ ***versus the number of segments NS for the circle.***

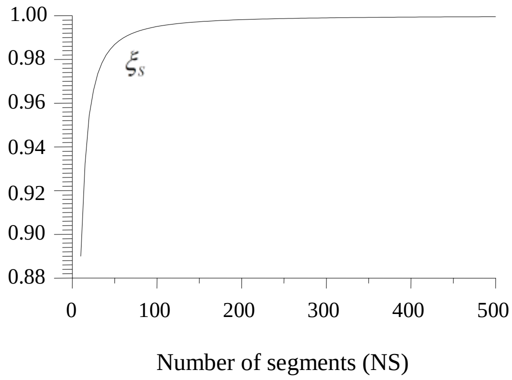

Fig. 16 - Variation of ξ_S ***versus the number of segments NS for the circle.***

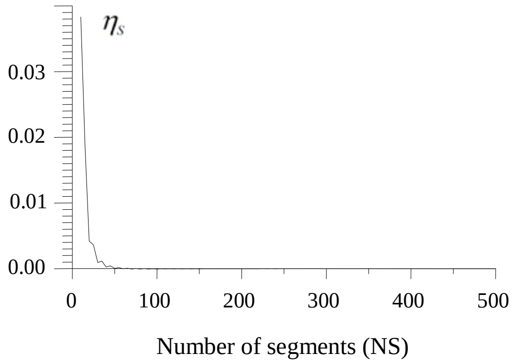

Fig. 17 - Variation of η_S ***versus the number of segments NS for the circle.***

The variation of shear stress along the wall of a circle for some values of S_x and S_y are shown in Figures 18, 19 and 20. In these examples, we took NS=10000. Then for each value of S_x and S_y may have a distribution of shear stress.

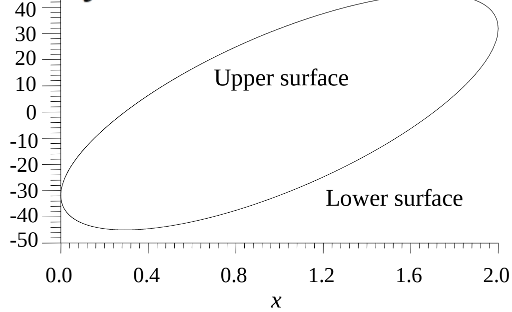

Fig. 18 - Variation of the shear stress along the wall circle for Sx=1.0 and Sy=1.0.

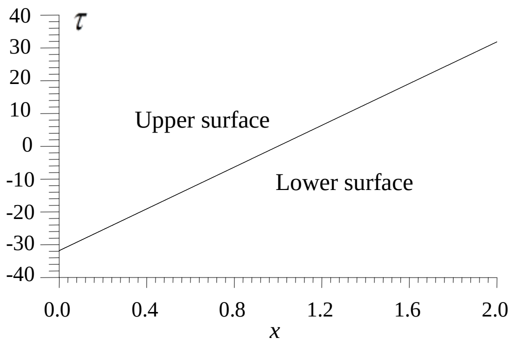

Fig. 19 - Variation of the shear stress along the wall circle for Sx=0.0 and Sy=1.0.

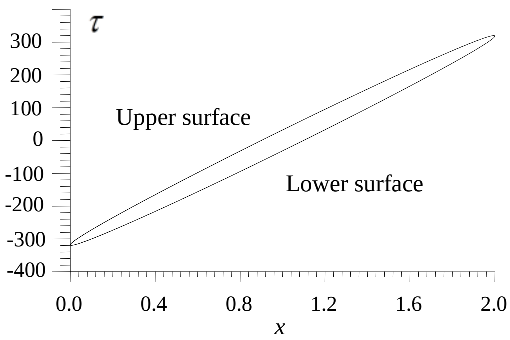

Fig. 20 - Variation of the shear stress along the wall circle for Sx=0.0 and Sy=10.0.

The second example chosen is that the airfoil DOUGLAS LA 203A with C=1.0. For this example we always take the thickness t=0.01.

The variation of the shear stress for this airfoil for different values of S_x and S_y are shown in Figures 21, 22 and 23.

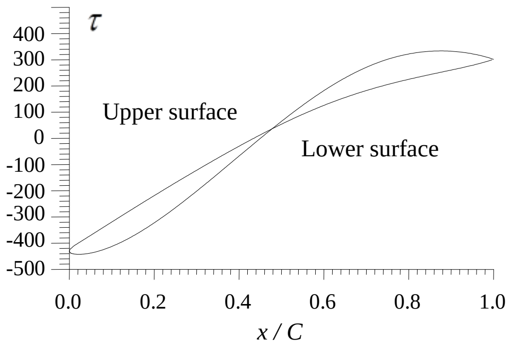

Fig. 21 - Variation of the shear stress along the wall of the airfoil DOUGLAS LA203A when Sx=0.0 and Sy=1.0.

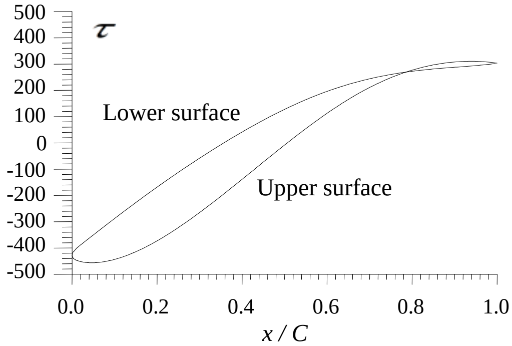

Fig. 22 - Variation of the shear stress along the wall of the airfoil DOUGLAS LA203A when Sx=1.0 and Sy=1.0.

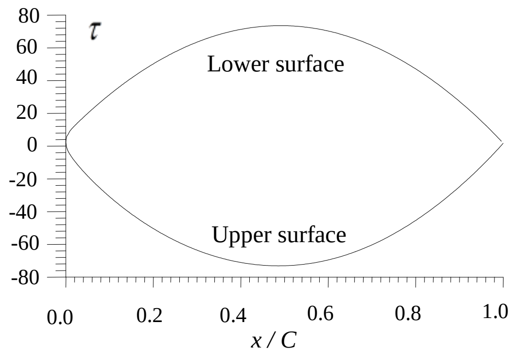

Fig. 23 - Variation of the shear stress along the wall of the airfoil DOUGLAS LA203A when Sx=1.0 and Sy=0.0.

The figure 24 shows the variation of the maximum value of $\tau^{+}_{\max}$ et $\tau^{-}_{\min}$ versus S_x and S_y. So, the more vertical shear S_y is large, more $\tau^{+}_{\max}$ et $\tau^{-}_{\min}$ becomes high.

The figure 25 shows the variation of the maximum value of $\tau^{+}_{\max}$ et $\tau^{-}_{\min}$ versus S_x when S_y=0.0. This figure is the compliment of Figure 24. In this case $\tau^{+}_{\max}$ is almost equal to $\tau^{-}_{\min}$ in absolute value.

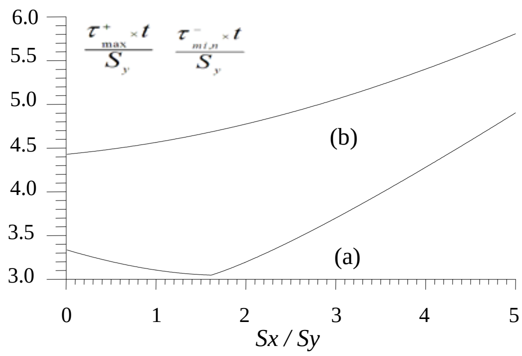

(a) : Variation of $(\tau^{+}_{\max} \times t)\ /\ S_y$ **.**

(b) : Variation of $(-\tau^{-}_{\min} \times t)\ /\ S_y$.

Fig. 24 - Variation of $(\tau^{+}_{\max} \times t)\ /\ S_y$ ***and*** $(-\tau^{-}_{\min} \times t)\ /\ S_y$ ***versus*** S_x / S_y ***for the airfoil DOUGLAS LA203 A.***

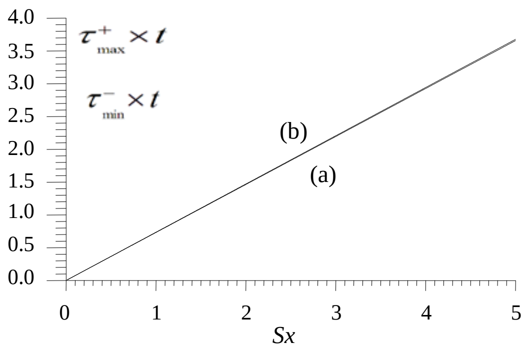

(a) : Variation of $\tau^{+}_{\max} \times t$

(b) : Variation of $-\tau^{-}_{\min} \times t$

Fig. 25 - Variation of $\tau^{+}_{\max}$ ***et*** $(-\tau^{-}_{\min})$ ***versus S***$_x$ ***when S***$_y$***=0.0 for the airfoil DOUGLAS LA 203 A.***

6.2 Results for different airfoils

The values in tables 4 and 5 are obtained for a discretization of one million points on the boundary of the airfoil when Sx=Sy=1.0. The thickness is taken to be t/C=0.01.

Moments and product of inertia Ixx, Iyy and Ixy are presented in references [7].

The airfoils selected in this publication regarding all airlines. It took 33 airfoils as presented in the table 4.

Airfoils that have ηS=0.0 mean that this airfoil is symmetrical. In this case, the shear center is located from the horizontal symmetry axis, inwardly a distance ξS relative to the leading edge. These results are found for the airfoil number 1 (NACA 0012), Number 5 (NACA 62), Number 6 (RAF 30), Number 17 (NACA M1) according to table 5.

The values of $\tau^{+}_{\max}$ et $\tau^{-}_{\min}$ depends on Sx and Sy. The airfoils which have a maximum, the greatest possible constraint is one that is in high demand airfoil. We find this case for the NACA M1 (number 17) profile. It is otherwise for the WORTMANN FX2 airfoil (number 16).

If the shear forces Sx and Sy in the center of shear presented in Table 5 are applied, it will not in this case the phenomenon of torsion.

Table 4 - References of the airfoils and the value of the shear stress $\tau_{S,0}/t$ at the opening airfoils.

N°	Airfoils names	$\tau_{S,0}/t$
1	NACA0012	4.425044
2	NACA 63-412	4.279588
3	RAE 2822	4.397287
4	NACA 0010-34	5.578217
5	NACA 62	4.472229
6	RAF 30	4.186719
7	E-385	4.646177
8	NACA 23009	5.845371
9	NACA 2412	4.357741
10	NASA AMES A-01	5.113134
11	AQUILA 9.3%	5.208383
12	AVISTAR	3.770983
13	CHEN	3.949288
14	FAUVEL 14%	3.752219
15	EIFFEL 385	3.742358
16	WORTMANN FX 2	2.693112
17	NACA M1	8.688636
18	ONERA OA209	5.719238
19	OAF 128	3.967910
20	ONERA NACA CAMBRE	4.711216
21	NASA LANGLEY RC-08 B3	6.772725
22	NASA LANGLEY RC-08 N1	6.794713
23	TRAINER 60	2.898697
24	TSAGI 8%	6.743970
25	TSAGI 12%	4.564709
26	EPPLER 520	3.462827
27	EPPLER 635	4.647121
28	LOCKHEED L-188 ROOT	3.814667
29	NACA 63-415	3.460841
30	NACA 63-210	5.188818
31	NACA 64-108	6.629517
32	NASA LANGLEY 64-012	4.443705
33	DOUGLAS LA203A	3.030211

Table 5 - Stress maximum and the position of the shear center of some airfoils.

N°	$\tau^{+}_{\max} \times t$	$-\tau^{-}_{\min} \times t$	ξ_S	η_S
1	4.52045	5.97929	0.26271	0.00000
2	4.30303	6.16136	0.28294	-0.02562
3	4.39762	5.90114	0.29757	-0.00473
4	5.57882	6.66320	0.37108	-0.01610
5	4.57211	6.00023	0.27083	0.00000
6	4.29871	5.72350	0.25998	0.00000
7	5.37088	7.66141	0.48236	-0.05314
8	5.87193	8.16689	0.24929	-0.01736
9	4.35786	5.96744	0.26520	-0.02452
10	5.13433	6.76407	0.28596	-0.01637
11	5.30166	7.65885	0.25105	-0.04905
12	3.77942	4.92719	0.30335	-0.02657
13	3.95733	6.05067	0.21267	-0.05685
14	3.98370	5.65741	0.20043	-0.02052
15	3.83989	5.70550	0.29287	-0.06941
16	2.71198	3.33076	0.38476	-0.03429
17	8.71315	11.20230	0.29570	0.00000
18	5.78284	7.79007	0.27693	-0.01452
19	3.97155	6.30563	0.20024	-0.01207
20	4.77201	6.29418	0.27596	-0.01287
21	6.79972	8.29754	0.34428	-0.01264
22	6.83759	9.07613	0.29337	-0.01759
23	3.04167	4.19153	0.28811	-0.00042
24	6.78046	8.82729	0.29785	-0.01418
25	4.62205	5.95387	0.30307	-0.02083
26	3.66332	4.84449	0.25938	0.00000
27	4.81587	6.61000	0.24172	-0.02480
28	3.81757	5.00155	0.41267	-0.02385
29	3.48340	4.98324	0.27203	-0.02559
30	5.18989	7.41203	0.26124	-0.01302
31	6.64367	9.17045	0.26857	-0.00660
32	4.61766	6.15478	0.26559	0.00000
33	3.10454	4.56410	0.33329	-0.06192

7 Conclusion

This work allows us to determine the distribution of shear stress in closed tubes, thin-walled mono box and made an application to the airfoils used in the field of aeronautics. Can be drawn from this work the following points:

- The discretization is done by straight line segments on the boundary of the section.
- Applications are made for values less than or equal to 0.01 for the thickness.
- To study a closed section must be an opening in this section in any location, and to study first, the stress distribution in the open section.
- We must determine the value of the shear stress in the point of opening of the closed sections.
- The shear stress is applied tangentially to the wall.
- A very important parameter that can be considered to calculate the shear stress appointed by shear flow.
- Section should be set in the reference mark through the center of gravity of the section.
- Determining center of gravity of the section is necessary.
- The calculation of the moments and product of inertia must be made with respect to the central axis.
- All airfoils considered are presented in tabulated values. The cubic spline interpolation is used in this case to obtain an analytic function of the upper and lower surface.
- The airfoils studied involving only the field of incompressible and compressible subsonic and transonic area.
- The discretization of the domain can be done with any number of segments. Application is made for a discretization of one Million segments.

- Condensation nodes to the leading edge of the airfoil is used to refine the points to the edge having the large curvature in this region.
- The application of shear to the shear center allows for the elimination of the twisting section.
- The position of the shear center does not depend on the value and position of the application of shear.
- As prospects. We can study the distribution of shear stress in sections multi boxes. Applications can be made for three boxes with and without effect of stiffeners (booms). In this case we must make an opening in each box, which it has its own constraints. $\tau_{S,0}$.

Acknowledgements

The authors acknowledge Khaoula, AbdelGhani Amine and Ritadj Zebbiche and Mouza Ouahiba for granting time to prepare this manuscript.

Appendix A. Nomenclature

(x_i, y_i)	Coordinates of a node.
NS	Number of segments.
NN	Number of nodes on the boundary of the section.
I_x , I_y	Central moments of inertia of the section.
I_{xy}	Central product of inertia of the section.
S_x	Horizontal shear.
S_y	Vertical shear.
q_b	Shear flow in the open tube.
q_s	Shear flow in the closed tube.
$q_{s,0}$	Value of shear flow at the opening.
τ	Shear stress.
$\tau_{s,0}$	Value of the shear stress at the opening.
T	Pitching moment.
L	Total length of the section.
d	Lever arm.
η^*	Normalized variable.
P , Q	Parameters for the control of mesh points (Stretching function).
C	Chord of the airfoil.
t	Thickness of the segment and the airfoil.
ξ_S, η_S	Coordinates of the shear center.
(x_O, y_O)	Position of point for calculation of moment.
E	Accuracy.

REFERENCES

[1]- T.H.G. Megson, Structures and Stress Analysis, 2nd edition, Butterworth-Heinemann, 2005.
[2]- T.H.G. Megson, Aircraft Structures for Engineering Students, 4th edition, Butterworth-Heinemann, 2007.
[3]- I.H. Abbott, A.E. Von Doenhoff, Theory of wing sections: Including a summary of Airfoil data, Dover Publications, Inc., New York, 1959.
[4]- C.A.J. Fletcher, Computational Techniques for Fluid Dynamics, Volume II, Specific Techniques for Different Flow Categories, Springer-Verlag, 1988.
[5]- A. Ralston, P. Rabinowitz, A First Course in Numerical Analysis, Dover Publications Inc., 2003.
[6]- B.P. Demidovitch, I.A. Maron, v. Polonski, Eléments de Calcul Numérique, 2nd edition, Edition Mir Moscou, 1987.
[7]- T. Zebbiche, M. Boun-jad, A. Allali, Geometric characteristics of thin wall sections with application to airfoils, Arab. J. Sci. Eng., 39(8) (2014) 5917-5927.